

Discrimination of Human Cell Lines by Infrared Spectroscopy and Mathematical Modeling

Rezvan Zendehtdel^a and Farshad H. Shirazi^{b,c*}

^aDepartment of Occupational Hygiene, School of Public Health, Shahid Beheshti University of Medical Sciences, Tehran, Iran. ^bSBMU Pharmaceutical Research Center, Tehran, Iran. ^cDepartment of Toxicology and Pharmacology, School of Pharmacy, Shahid Beheshti University of Medical Science, Tehran, Iran.

Abstract

Variations in biochemical features are extensive among cells. Identification of marker that is specific for each cell is essential for following the differentiation of stem cell and metastatic growing. Fourier transform infrared spectroscopy (FTIR) as a biochemical analysis more focused on diagnosis of cancerous cells.

In this study, commercially obtained cell lines such as Human ovarian carcinoma (A2780), Human lung adenocarcinoma (A549) and Human hepatocarcinoma (HepG2) cell lines in 20 individual samples for each cell lines were used for FTIR spectral measurements. Data dimension were reduced through principal component analysis (PCA) and then subjected to neural network and linear discrimination analysis to classify FTIR pattern in different cell lines.

The results showed dramatic changes of FTIR spectra among different cell types. These appeared to be associated with changes in lipid bands from CH₂ symmetric and asymmetric bands, as well as amide I and amid II bands of proteins. The PCA-ANN analysis provided over 90% accuracy for classifying the spectrum of lipid section in different cell lines. This work supports future study to establish the data bank of FTIR feature for different cells and move forward to tissues as more complex systems.

Keywords: Cell line; Discrimination; Fourier transform infrared; Artificial neuronal network; Linear discriminate analysis.

Introduction

The regulation of gene expression is various among cells in both normal and pathological specimen (1). These sources of variation causes different biochemical matrix in cells which are relevant for different studies (2-4).

Monitoring of the stem cell differentiation (5) need careful and complex laboratory protocols of assays including those of immunocytochemistry

on cells (6, 7). These protocols require expert personals and is time consuming and expensive. Moreover, in this processes limited numbers of biomarkers exist (8, 9). There is a clear need for a truly technique to follow up the map of differences in various cells. The purpose and potency of this approach is to evaluate the preparation of spectrum bank for different cells, which might well be used as a discrimination and identification fingerprint for different cells in the future.

There is an increasing interest in the use of FTIR to a large number of different applications

* Corresponding author:

E-mail: f.shirazi@sbm.ac.ir

such as screening of MDR phenotype cells (13) and diagnosis of normal and malignant cells including ovarian (14), prostate (15), lung (16), colon (17). Although FTIR spectroscopy was recognized as a potential useful method in cancer research, it has not yet complete different fields of biomedical applications and diagnosis research.

In order to explain complex information from FTIR spectra, it is necessary to use mathematical analysis. Various algorithms have been created to classify tumor cells (18). Most of these methods have led to the development of analytical instruments that are currently approved by the Food and Drug Administration for the routine screening of gynecologic smears (19, 20). Multiple studies during the past five decades have developed multivariate analysis of data (21-23). Advanced mathematical systems included Neural networks as non-linear analysis and linear discriminate analysis as linear statistical data modeling tools could be find patterns of data (24).

In this research, we used a FTIR-based assay followed by multivariate analysis to look for the cell specific patterns. Principal component analysis (PCA) has been employed as a data dimension reduction model. Reduced data matrix was forwarded to linear discriminate analysis (LDA) and artificial neuronal network (ANN) as most recent developed models to discriminate different cell lines.

Experimental

Cell lines

A2780 (human ovarian carcinoma) and A549 (human lung carcinoma) and HepG2 (human liver carcinoma) cell lines were obtained from Pasture Institute National Cell Bank of Iran (Tehran, Iran). All cell lines were grown in RPMI-1640 medium and supplemented with 10% heat inactivated fetal bovine serum, antibiotics: penicillin, streptomycin (all chemicals from Sigma). Cells were maintained at 37 °C in humidified atmosphere containing 5% CO₂. All cells have been used at almost the same life time *i.e.* after two passages.

Cell preparation for spectroscopy

The following procedure was similarly applied

for all cell lines. Cells were trypsinized from the original flask and seeded in 25 cm² flasks with fresh medium to reach the logarithmic phase of growth curve. After that cell were washed twice in saline (0.9% NaCl), suspend and centrifuged at 1000 rpm for 5 min, then resuspended in saline to obtain a concentration of 1×10^5 cells. 10 μ L of each cell suspension was placed on a zinc selenide sample carrier which was dehydrated in a vacuum cabin (0.8bar). These plates were then used for FTIR spectroscopy.

FTIR spectroscopy

For FTIR studies, thin dried films of cell suspension was used on the Zinc selenide window by using a WQF-510 (Rayleigh Optics, China) spectrometer, equipped with a KBr beam splitter and a DLaTGS (deuterated Lanthanide triglycine sulphate) detector. The whole system was continuously purged with N₂ (99.999%). In each spectrum, 100 scans were collected at a resolution of 4 cm⁻¹ for every wave number between 400 and 4000 cm⁻¹. These experimental conditions were kept constant for all measurements. Each single spectrum was baseline corrected and then all wave number normalized in order to better comparison for the range spanning from 0 to 1.

Recovery of drying technique

Drying of cells in vacuum of 0.8 bars for different times was assessed by FTIR analysis. Remained water in dehydrated sample was evaluated by Differential Scanning calorimetry analysis (DSC). Temperature program was changed from -20 to 100 °C with the rate of 5 °C/min.

Data analysis

Data set

For a better modeling a total of 60 FTIR spectrum (20 individual samples for each cell lines) between 1000-3000 cm⁻¹ have been used in this study as the dataset (25, 26) Distribution of different FTIR spectra was equal for A2780, A549 and HepG2 cell lines.

Principle component analysis

PCA is a well-known method of dimension reduction. The basic idea of PCA is to reduce

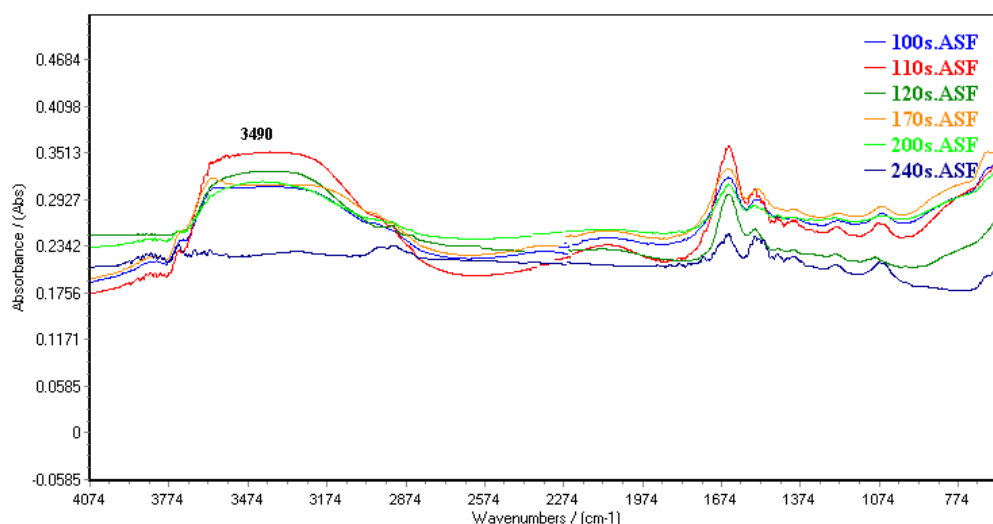


Figure 1. Spectral features of water in dehydrated cell suspension in a vacuum cabin (0.8bar) for different time.

the dimensionality of a data set, while retaining as much as possible the variation present in the original predictor variables. In mathematical terms, PCA maximizes the variance of a linear combination of the original predictor variables (27).

PCA scores from various PCs were examined to give best separation between cell lines. PCA was used for preliminary data reduction and then output processed with artificial neural networks (ANN) and linear discrimination analysis (LDA).

Artificial neural networks

Artificial neural networks (ANN) are computerized mathematical models designed to mimic the architecture of the brain. They are able to detect non linearity, making them capable of learning and adaptability (28). The network include of unites named neurons. Neurons are organized in parallel layers: input, hidden (single or multiple), and output. Each neuron connects to all neurons of another layer but not to those in the same layer. Neurons process the data using a variety of mathematical functions (24).

Multiple layer perception neuronal networks were designed according to MATLAB. The output of PCA analysis has been used for input layer of ANN model. The output layer consisted of three output neurons, one to classify the A549 category and the others for HepG2, and A2780 data.

Linear discriminate analysis

The basic theory of linear discriminate analysis is to classify the dependent variable by dividing an n-dimensional space into two regions that are separated by a hyperplane (27). The data were analyzed with multivariate LDA analysis using the cell types as the dependent variable and the output of PCA analysis as independent variables.

Results

Recovery of drying technical

10 μ L of A2780 cell suspension was placed on a zinc selenide sample carrier which was dehydrated in a vacuum cabin (0.8bar) for different time. Figure 1 shows FTIR spectrum of dehydrated cells in different time. Water band at 3490 cm^{-1} was omitted in 4 min of vacuum drying. The remained water in dehydrated cell suspension was estimated by DSC analysis (Figure 2). There is a reaction at approximately 0 $^{\circ}\text{C}$ could be related to fuse of ice crystal in samples. The results specified 2.7 ± 0.59 % of water remained in dehydrated samples.

Spectrum alteration

Figure 3 shows typical FTIR spectra for A2780, A549 and HepG2 cell lines from the region of 1800-900 cm^{-1} . These spectra represent average spectra from the 20 individual of the same cells. The normalized FTIR spectra in this

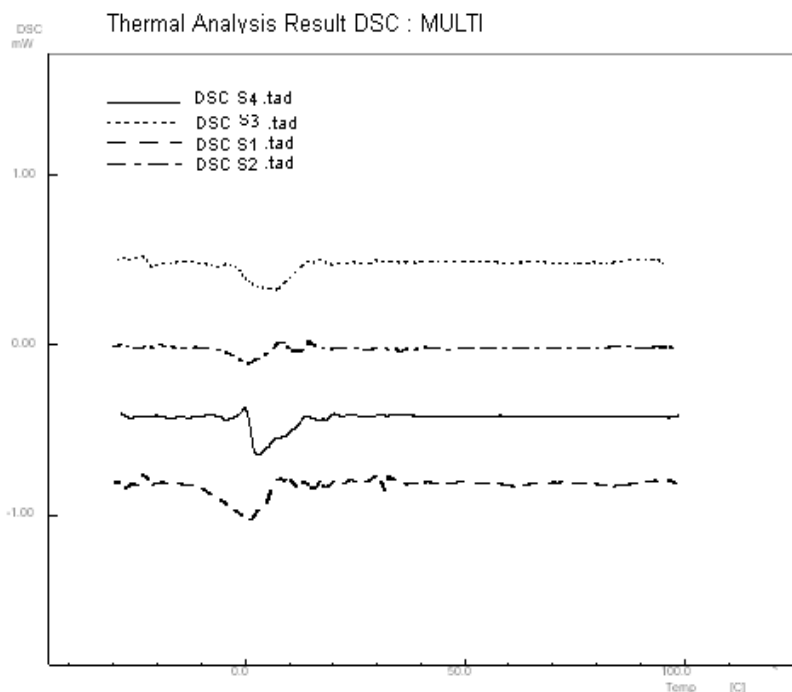


Figure 2. DSC analysis of dehydrated cell suspension.

region showed alterations in different spectrum areas. There is a peak about 1636 cm^{-1} in the spectra of the three cell lines. This peak is attributed amid I structure (30) where connected to a shoulder at 1620 cm^{-1} for A549 and HepG2 cell lines.

The normalized FTIR spectra of A2780, A549 and HepG2 cell lines are shown between $3100\text{--}2500\text{ cm}^{-1}$ in Figure 4. CH_2 symmetric and asymmetric stretching vibration bands are appeared at 2920 and 2852 cm^{-1} , respectively

(25). The results showed CH_2 symmetric and asymmetric stretching vibration bands shift to higher wave numbers in A549 cells. Moreover, CH_3 stretching vibrations bands at 2950 cm^{-1} (30) are appeared in higher positive feature for A2780 cells.

PCA-ANN modeling

The five regions were defined as follows : fatty acids from 2500 to 3000 cm^{-1} , mixed region from 2000 to 2500 , Proteins from 1500 to 2000

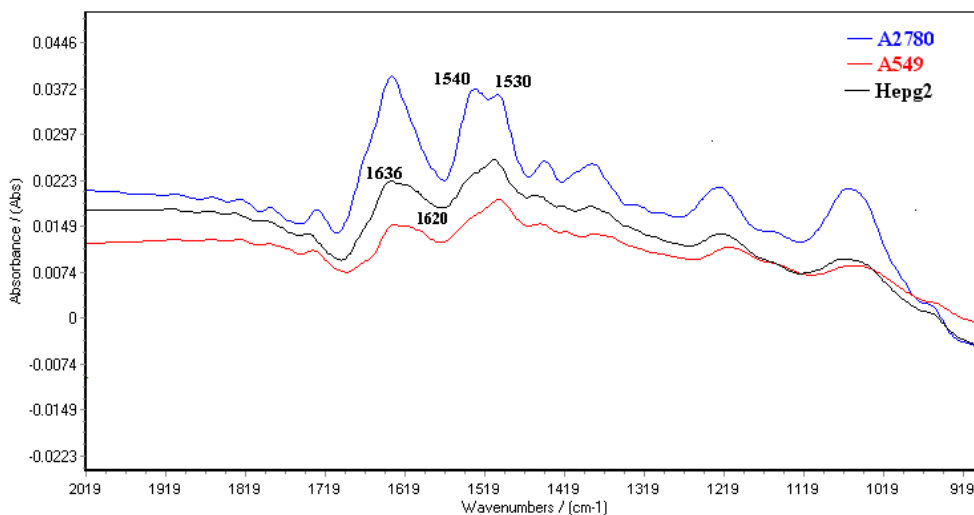


Figure 3. Spectral features of A2780, A549 and HepG2 cell lines in the FTIR spectral region of $1800\text{--}900\text{ cm}^{-1}$.

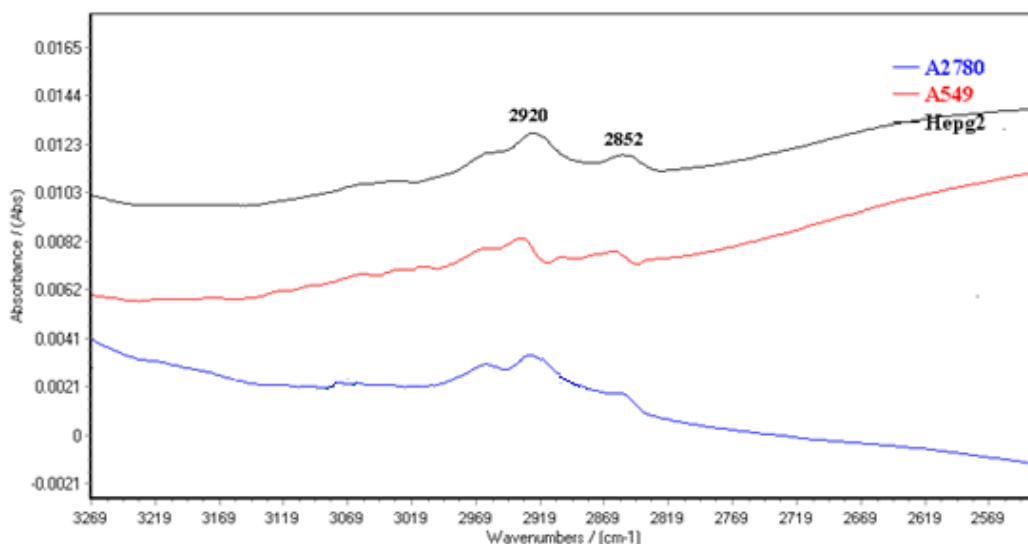


Figure 4. Spectral features of A2780, A549 and HepG2 cell lines in the region of 3100-2500 cm^{-1} .

cm^{-1} and typing region from 1000 to 1500 cm^{-1} (29). FTIR data of A2780, A549 and HepG2 cell lines were sorted randomly into 20 different data sets (numbered 1 to 20) each composed of 45 training variables (include 35 training data and 10 validation data) and 15 testing variables. The 20 models were analyzed with PCA-ANN model where classification results are shown in Table 2. Models 1 to 5 use all FTIR wave number from 1000 to 3000 cm^{-1} , while models 6 to 20 used the four segmentation of FTIR wave number from 1000-1500 cm^{-1} , 1500-2000 cm^{-1} , 2000-2500 cm^{-1} and 2500-3000 cm^{-1} .

We applied ANN on the dataset using Feed-forward backpropagation to analyze our networks. Training algorithms was obtained using Levenbery-Marqwardt back propagation algorithm. Three-layer neural networks was set, include one output layer, one hidden layer and an input layer. In order to determine the well

optimized structure of the networks, error goal was selected 0.001% and verify number of hidden neurons were constructed. The parameters of the optimized neural network are listed in Table 1.

When the model is performed for the training dataset in present investigation, Cell lines pattern of each experiment in the testing dataset is predicted in turn using the learned rules derived from the training dataset. The results indicate that PCA-ANN can be tested to correctly classify fatty acids spectra with the mean of 90.12 ± 4.02 based on the FTIR data set (Table 2).

PCA-LDA modeling

PCA-LDA was used to analyze the same 20 data sets, using FTIR spectra values. The results of these analyses are given in Table 2. Correct classification rates provided by the LDA models were variable between 70% to 90%. Comparison of the 20 LDA models indicates that the variation

Table1. Optimized neuronal network parameters.

Error goal	0.001
Transfer function of hidden layer	logsig
Number of hidden nodes	15
Training algorithm	Levenbery-Marqwardt
mu	0.001
Mu increase	10
Mu decrease	0.1
Epoch number	30

Table2. Classification of FTIR data set of test (n=15; 5 A2780,5 HepG2 and 5 A549) by PCA-LDA and Artificial Neural Network.

	Model Train cell lines (<i>n</i> =45; 15 A2780 and 15 HepG2,15 A549)	Principle component analysis-Artificial neural network	Principle component analysis-Linear discriminate analysis
		percent of correctly classified cell lines	percent of correctly classified cell lines
Models trained with variables in 1000-3000 cm ⁻¹			
Seri 1	1	80	85
	2	90	90
	3	83	85
	4	88.37	82
	mean	85.34 ± 4.6	85.5 ± 3.3
Models trained with variables in 3000-2500 cm ⁻¹			
Seri 2	5	95.8	85
	6	90	90
	7	86.67	85
	8	88	80
	mean	90.12 ± 4.02	85 ± 4
Models trained with variables in 2500-2000 cm ⁻¹			
Seri 3	9	85.67	73
	10	81.67	80
	11	79.86	75
	12	75.67	70
	mean	80.72 ± 4.14	74.5 ± 4.2
Models trained with variables in 1500-2000 cm ⁻¹			
Seri 4	13	83.33	86
	14	85	85
	15	90	80
	16	88.37	83.34
	mean	86.68 ± 3.06	83.58 ± 2.6
Models trained with variables in 1000-1500 cm ⁻¹			
Seri 5	17	93.33	85
	18	86.67	85
	19	80	80
	20	85	78.3
	mean	83.25 ± 5.5	82 ± 3.4

of prediction rate between the members of protein region is lower than others. Because of more accuracy, PCA-LDA is a better model for discrimination of total FTIR region than other models.

Comparison of PCA-LDA and PCA- ANN

The comparison of PCA-LDA and PCA-ANN was done using the paired student t-test. From the result of t-test, it is obvious that the difference of prediction accuracy in PCA-ANN

models in comparison with the accuracy of PCA-LDA models is substantial with p-value ≤ 0.01.

Discussion

Determination of cell-types with immunocytochemistry methods has been reported frequently (6-8). This study was based on the need to apply a noninvasive and inexpensive technique for recognizing different cells. FTIR as a reliable method was

used for diagnosis of different abnormal cells (32). Mathematical algorithms was applied by authors to analyze the complex dataset of FTIR spectrum. Andreas Lux was investigated FTIR spectroscopy AND ANN model to diagnosis Hereditary Hemorrhagic Telangiectasia disease (33). They used supervised model to classify groups. In our study PCA model was applied before ANN algorithm to reduce the dimension of dataset. Data reduction could be simplify model and facilitate finding of data pattern. In the often researches total area of FTIR spectrum (400-4000 cm^{-1}) was investigated (34,35). In this study FTIR spectrum was divided to four section(Fatty acid, mixed region, proteins and typing region)and each region was analyzed separately for better discussing .

Although cellular biomolecules are varied but thorough a spectroscopy analysis, such as FTIR, may be capable of detecting these variations as early as in the first hours of sampling. Sixty individual FTIR spectra of A2780, A549 and Hepg2 cell lines forwarded to supervised models for finding pattern of cells. Since several studies used FTIR analysis in cell biology (14-17), one of the potential approaches in this study is assessment of drying recovery and repeatability. Spectral features of water band in vacuum process are flatted after 4min drying. The results of DSC analysis confirm drying reparability in dehydrated samples with a suitable recovery.

The results exhibited dramatic change as marker for cell-type identification. There is a peak about 1636 cm^{-1} in the spectra of the three cell line related to β -sheet secondary structure of amid I (30) where connected to a positive shoulder at 1620 cm^{-1} in two cell lines but not in the ovarian cell. The bands at 1620 cm^{-1} are assigned to aggregated strand structures of amid I (29). Moreover CH₂ symmetric and asymmetric stretching vibration bands shift to higher wave numbers in A549 cells. These critical wave numbers is suggested as cell difference in visual judgment.

PCA-ANN model classifies different FTIR region between 85% to 93% correctly. Comparison of the 20 PCA-ANN models indicates that uses of variable in the region of 2500-3000 cm^{-1} is more accurate than the others when 95% of FTIR data set was anticipated

exactly. From our results correct classification provided by the PCA-LDA models were less accurate than those provided by PCA-ANN analysis. Our results demonstrate that it is possible to classify different cell lines based on the analysis of FTIR spectra markers using multivariate PCA-ANN model.

As is shown in our results, FTIR data set between 1500-2000 cm^{-1} was classified as a data region with less variability among different series, and therefore very much suitable for the discrimination of different cell lines using both PCA-ANN and PCA-LDA models. It is therefore acceptable to conclude that this segment of FTIR data, which related to protein structure of cells (31), is a good candidate for the discrimination of different cell lines by FTIR and various mathematical models.

References

- (1) Whitehead A and Crawford LD. Variation in tissue-specific gene expression among natural populations. *Genome Biol.* (2005) 6: 13-18.
- (2) Oleksiak MF, Churchill GA and Crawford DL. Variation in gene expression within and among natural populations. *Nat. Genet.* (2002) 32: 261-266.
- (3) Silberstein GB and Daniel CW. Investigations of mouse mammary ductal growth regulation using slow release implants. *J. Dairy Sci.* (1987) 70: 1981-1990.
- (4) Raccurt M, Tam SP, Lau P and Mertani H. Suppressor of cytokine signalling gene expression is elevated in breast carcinoma. *Br. J. Cancer.* (2003) 89: 524-532.
- (5) Segers V and Lee F. Stem-cell therapy for cardiac disease. *Nature* (2008) 451: 937-942.
- (6) Adina AB, Goenadi FA, Handoko FF, Nawangsari DA, Hermawan A, Jenie RI and Meiyanto E. Combination of ethanolic extract of citrus aurantifolia peels with doxorubicin modulate cell cycle and increase apoptosis induction on MCF-7 cells. *Iran. J. Pharm. Res.* (2014) 13: 919-926.
- (7) Nagano K, Yoshida Y and Isobe T. Cell surface biomarkers of embryonic stem cells. *Proteomics* (2008) 8: 4025-4035.
- (8) Haarmann A, Dei A, Prochaska J, Foerch C and Weksler B. Evaluation of soluble junctional adhesion molecule-a as a biomarker of human brain endothelial barrier breakdown. *PLoS ONE* (2010) 5: 1-10.
- (9) German M, Pollock H and Zhao B. Characterization of putative stem cell populations in the cornea using synchrotron infrared microspectroscopy. *Invest. Ophthalmol. Visual Sci.* (2006) 47: 2417-2421.
- (10) Krafft C, Sobottka B and Geiger D. Classification of malignant gliomas by infrared spectroscopic imaging and linear discriminant analysis. *Anal. Bioanal. Chem.*

- (2007) 387: 1669-1677.
- (11) Steller W, Einkenel J and Horn LC. Delimitation of squamous cell cervical carcinoma using infrared microspectroscopic imaging. *Anal. Bioanal. Chem.* (2006) 384: 145-154.
- (12) Afrakhteh M, Khodakarami N, Moradi A, Alavi E and Hosseini Shirazi F. A study of 13315 papanicolau smear diagnoses in shohada hospital. *J. Family Reproduct. Health* (2007) 1: 75-79.
- (13) Jean-Marc KG, Morjani H and Manfait M. Ultrastructural Appraisal of the multidrug resistance in k562 and Ir73 cell lines from fourier transform infrared spectroscopy. *Cancer Res.* (1993) 53: 3681-3686.
- (14) Mehrotra R, Tyagi G, Jangir D, Dawar R and Gupta N. Analysis of ovarian tumor pathology by Fourier Transform Infrared Spectroscopy. *J. Ovarian Res.* (2010) 3: 27-33.
- (15) Kwak J, Hewitt SM, Sinha S and Bhargava R. Multimodal microscopy for automated histologic analysis of prostate cancer. *BMC Cancer* (2011) 11: 62-70.
- (16) Lewis P, Lewis KE, Ghosal R and Bayliss S. Evaluation of FTIR Spectroscopy as a diagnostic tool for lung cancer using sputum. *BMC Cancer* (2010) 10: 640-650.
- (17) Xiang L, Qing-Bo L, Zhang G and Xu Y. Identification of colitis and cancer in colon biopsies by fourier transform infrared spectroscopy and chemometrics. *Scientific World J.* (2012) 2012: 936149.
- (18) Johnson HE, Broadhurst D, Kell DB and Theodorou MK. High-throughput metabolic fingerprinting of legume silage fermentations via fourier transform infrared spectroscopy and chemometrics. *American Society for Microbiol.* (2004) 70: 1583-1592.
- (19) Cenci M, Nagar C and Vecchione A. PAPNET-assisted primary screening of conventional cervical smears. *Anticancer Res.* (2000) 20: 3887-3889.
- (20) Troni GM, Cipparrone I, Cariaggi MP and Ciatto S. Detection of false-negative Pap smear using the PAPNET system. *Tumori.* (2000) 86: 455-457.
- (21) Ellis DI, Broadhurst D, Kell DB, Rowland JJ and Goodacre R. Rapid and quantitative detection of the microbial spoilage of meat by fourier transform infrared spectroscopy and machine learning. *American Society for Microbiol.* (2002) 68: 2822-2828.
- (22) Marchevsky AM, Tsou JA and Laird-Offringa IA. Classification of individual lung cancer cell lines based on dna methylation markers. *J. Molecular Diagnostics* (2004) 6: 28-35.
- (23) Marchevsky AM, Patel S, Wiley KJ, Stephenson MA, Gondo M and Brown RW. Artificial neural networks and logistic regression as tools for prediction of survival in patients with stages I and II non-small cell lung cancer. *Med. Pathol.* (1998) 11: 618-625.
- (24) Goodacre R, Neal MJ and Kell DDB. Rapid and quantitative analysis of the pyrolysis mass spectra of complex binary and tertiary mixtures using multivariate calibration and artificial neural networks. *Analytical Chem.* (1994) 66: 1070-1085.
- (25) Essendoubi M, Toubas D, Lepouse C and Leon A. Epidemiological investigation and typing of *Candida glabrata* clinical isolates by FTIR spectroscopy. *J. Microbiol. Methods* (2007) 71: 325-331.
- (26) Khanmohammadi M, Nasiri R, Ghasemi K, Samani S and Garmarudi A. Diagnosis of basal cell carcinoma by infrared spectroscopy of whole blood samples applying soft independent modeling class analogy. *J. Cancer Res. Clin. Oncol.* (2007) 133: 1023-1030.
- (27) Jahandideh S and Abdolmaleki P. Prediction of melatonin excretion patterns in the rat exposed to ELF magnetic fields based on support vector machine and linear discriminant analysis. *Micron.* (2010) 41: 882-885
- (28) Farid EA. Artificial neural networks for diagnosis and survival prediction in colon cancer. *Molecular Cancer* (2005) 4: 1-12.
- (29) Baker MJ, Gazi E, Brown MD and Shanks JH. FTIR-based spectroscopic analysis in the identification of clinically aggressive prostate cancer. *British J. Cancer* (2008) 99: 1859-1866.
- (30) Zanier K, Ruhlmann C and Melin F. E6 proteins from diverse Papillomaviruses self-associate both *in-vitro* and *in-vivo*. *J. Molecular Biol.* (2010) 396: 90-104.
- (31) McCann MC, Defernez M and Urbanowicz BR. Neural network analyses of infrared spectra for classifying cell wall architectures. *Plant Physiol.* (2007) 143: 1314-1326.
- (32) Jiang QQ, Zhao YP, Gao WY, Li X, Huang LQ and Xiao PG. Isolation, purification, characterization and effect upon hepg2 cells of anemaran from rhizome anemarrhena. *Iran. J. Pharm. Res.* (2013) 12: 777-788.
- (33) Lux A, Müller R, Tulk M, Olivieri C, Zarrabeita R, Salonikios T and Wirmitzer B. HHT diagnosis by Mid-infrared spectroscopy and artificial neural network analysis. *Orphanet J. Rare Dis.* (2013) 8: 94-105.
- (34) Mackanos MA, Hargrove J, Du CB, Friedland S and Soetikno RM. use of an endoscope compatible probe to detect colonic dysplasia with Fourier Transform Infrared (FTIR) spectroscopy. *J. Biomed. Opt.* (2009) 14: 44006.
- (35) Wood BR, Chiriboga L, Yeec H, Quinn MA, McNaughton D and Diema M. Fourier transform infrared (FTIR) spectral mapping of the cervical transformation zone, and dysplastic squamous epithelium. *Gynecol. Oncol.* (2004) 93: 59-68.

This article is available online at <http://www.ijpr.ir>